UC Santa Cruz
UC Santa Cruz Previously Published Works

Title

Biochemical and Cellular Characterization and Inhibitor Discovery of Pseudomonas aeruginosa 15-Lipoxygenase

Permalink

https://escholarship.org/uc/item/4kz0h0rg

Journal

Biochemistry, 55(23)

ISSN

0006-2960

Authors

Deschamps, Joshua D
Ogunsola, Abiola F
Jameson, J Brian
et al.

Publication Date

2016-06-14

DOI

10.1021/acs.biochem.6b00338

Peer reviewed

Biochemical/Cellular Characterization and Inhibitor discovery of *Pseudomonas aeruginosa* 15-Lipoxygenase

Joshua D. Deschamps[1,&], **Abiola F. Ogunsola**[2,&], **J. Brian Jameson II**[1,&], **Adam Yasgar**[3], **Becca A. Flitter**[2], **Cody J. Freedman**[1], **Jeffrey A. Melvin**[2], **Jason V.M.H. Nguyen**[1], **David J. Maloney**[3], **Ajit Jadhav**[3], **Anton Simeonov**[3], **Jennifer M. Bomberger**[2,*], **Theodore R. Holman**[1,*]

[1]Department of Chemistry and Biochemistry, University of California, Santa Cruz, CA 95064

[2]Department of Microbiology and Molecular Genetics, University of Pittsburgh, Pittsburgh, PA 15219

[3]National Center for Advancing Translational Sciences, National Institutes of Health, 9800 Medical Center Drive, MSC 3370, Bethesda, Maryland 20892, United States

Abstract

Pseudomonas aeruginosa is an opportunistic pathogen which can causes nosocomial and chronic infections in immunocompromised patients. *P. aeruginosa* secretes a lipoxygenase, LoxA, but the biological role of this enzyme is currently unknown. LoxA has poor sequence similarity to both soybean LOX-1 (s15-LOX-1) and human 15-LOX-1, 37% and 39%, respectively and yet has comparably fast kinetics to s15-LOX-1 (k_{cat} = 181+/−6 s^{-1} and k_{cat}/K_M = 16+/−2 $\mu M^{-1}s^{-1}$ at pH 6.5). LoxA is capable of efficiently catalyzing the peroxidation of a broad range of free fatty acid (FA) substrates (e.g. AA and LA) with high positional specificity, indicating a 15-LOX. Its mechanism is through a hydrogen-atom abstraction (kinetic isotope effect (KIE) greater than 30) and yet LoxA is a poor catalyst against phosphoester-FAs, suggesting that LoxA is not involved in membrane decomposition. LoxA also does not react with 5- or 15-HETEs, indicating poor involvement in lipoxin production. A LOX high-throughput screen of the LOPAC library yielded a variety of low micromolar inhibitors; however, none selectively targeted LoxA over the human LOX isozymes. With respect to cellular activity, LoxA expression is increased when *P. aeruginosa* transitions to a biofilm mode of growth, but LoxA is not required for biofilm growth on abiotic surfaces. However, LoxA does appear to be required for biofilm growth in association with the host airway epithelium, suggesting a role for LoxA in mediating bacterial-host interactions during colonization.

Graphical Abstract

*To whom correspondence should be addressed: Phone (831) 459-5884; Fax (831) 459-2935; tholman@chemistry.ucsc.edu. Phone (412) 624-1963; Fax (412) 624-2139; jbomb@pitt.edu.
&These authors contributed equally to the manuscript.
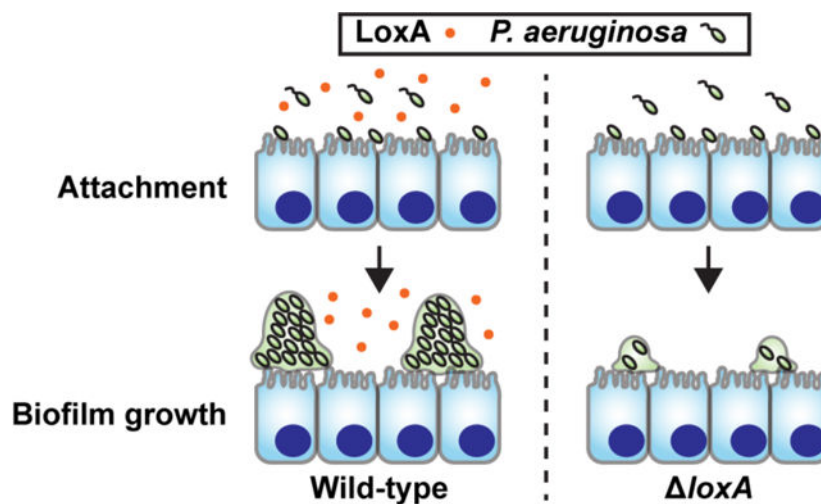
Pseudomonas aeruginosa (*P. aeruginosa*) is the second most prevalent cause of nosocomial pneumonia infections and a major cause of morbidity and mortality among cystic fibrosis (CF) patients.[1] Recent studies show that in (CF), the opportunistic pathogen *P. aeruginosa* is a major contributor to respiratory failure; it is the predominant airway pathogen in ~50% of patients, and present in another ~30% of patients.[2–4] Compounding its pathogenicity, *P. aeruginosa* has high intrinsic antibiotic resistance in the planktonic state and infections are often refractory to treatment.[5] During chronic infections, as is the case for a majority of CF patients, *P. aeruginosa* forms biofilms that further increase resistance to the point that they are virtually impossible to clear with existing antibiotics.[6–8] Contributing to the pathology in the CF airway, chronic bacterial infection induces vigorous inflammatory responses in the airways dominated by polymorphonuclear neutrophils and the potent inflammatory mediators that they release when activated.[9–13] This combination of chronic infection and uncontrolled inflammation in the CF airway leads to progressive lung damage, and eventually bronchiectasis, creating an urgent need for the identification of new therapeutic targets to combat chronic *P. aeruginosa* infections.

P. aeruginosa produces and secretes a functional 15-lipoxygenase (15-LOX),[14] whose transcription is up-regulated more than 200-fold during biofilm formation.[15] In addition, *P. aeruginosa* has been shown to activate cytosolic phospholipase A2 during infection, increasing the available pool of cytosolic and extracellular arachidonic acid (AA).[16] These data, coupled with the finding that exogenous 15-LOX can initiate anti-inflammatory signaling, suggest a role for *P. aeruginosa* 15-lipoxygenase (LoxA) in modulation of host-bacterial interactions.[17] Indeed, *P. aeruginosa* is not the only pathogen shown to possess 15-LOX activity. *Toxoplasma gondii* also expresses a 15-LOX enzyme that regulates host inflammatory processes during infection.[17] To investigate a potential role of LoxA in *P. aeruginosa* pathogenesis, further characterization of the effects of enzyme expression and function during the interaction of *P. aeruginosa* with the host during infection is needed.

The original characterization of LoxA verified the functionality of the enzyme and the localization to the periplasm and extracellular space, but did not delve into the kinetics or substrate specificity of the enzyme. In addition, the authors were unable to determine conditions that yielded significant native protein expression.[14] Since then, gene expression studies have found significant increases in mRNA levels of *loxA* expression when *P. aeruginosa* initiates biofilm formation.[15] Recombinant expression and purification have also been reported recently, allowing further kinetic characterization including temperature and pH activity profiles and product stereochemistry determination using the substrate linoleic acid (LA).[18] Herein, we performed a number of experiments to further characterize the enzyme activity, assess its reactivity with biologically relevant substrates, discover novel inhibitors, and investigate the role of LoxA in host colonization by *P. aeruginosa*.

Materials and Methods

Materials.

Commercial fatty acids were purchased from Nu Chek Prep, Inc. (MN, USA). Fatty acids used for the secondary products study were made by reacting arachidonic acid (AA) with human 5-LOX or soybean LOX15 to generate their respective HpETE or HETE products. Commercial fatty acids were further re-purified using a Higgins HAISIL column (5 μm, 250 × 10 mm) C-18 column. An isocratic elution of 85% A (99.9% methanol and 0.1% acetic acid): 15% B (99.9% water and 0.1% acetic acid) was used to purify the fatty acids. All HpETEs and HETEs generated for the secondary product study were purified using a Higgins HAISIL column (5 μm, 250 × 10 mm) C-18 column. An isocratic elution of 50% A (99.9% acetonitrile and 0.1% acetic acid): 50% B (99.9% water and 0.1% acetic acid) was used to purify the products. All fatty acids were tested for purity using LC-MS/MS and were found to have greater than 95% purity. Post purification, all fatty acids were stored at either −20 °C or −80 °C. Perdeuterated LA (d31-LA) (98% deuterated, Cambridge Isotope Laboratories) was purified as previously described.[19] All other chemicals were of high quality and were used without further purification.

Lipoxygenase (LOX) products were generated by reacting an individual substrate with LoxA in 500 mL of 25 mM HEPES (pH 7.0) with 50 μM substrate and run to completion. Reactions were quenched with 2.5 mL acetic acid, extracted three times with 30% volume of dichloromethane, evaporated to dryness, and reconstituted in methanol. The products were HPLC purified using an isocratic elution of 75% A (99.9% methanol and 0.1% acetic acid): 25% B (99.9% water and 0.1% acetic acid). The products were tested for their purity using LC-MS/MS and were found to have > 98 % purity.

P. aeruginosa wild type (PAO1) and knockout (PW3111) strains were obtained from the *P. aeruginosa* Mutant Library at The University of Washington.[20] Overexpression strain was a generous gift from Matthew Parsek. PA1169 (LoxA) and PA1168 were cloned as an operon with the native ribosomal binding site into the arabinose inducible vector pMJT-1. The resulting plasmid was transformed into PAO1 using 300 μg/mL carbenicillin for selection.

Recombinant Plasmid Construction.

Several methods to insert *loxA* into an *E. coli* expression plasmid were tried. First a PCR fragment was generated using Taq polymerase and cleaved with Xho1 and Nco1. pET28-a was treated with the same enzymes, then treated with calf intestinal phosphatase. Ligation between pET28-a and *loxA* gene was unsuccessful. The *loxA* gene was then inserted into pCR-XL-TOPO using the TOPO cloning kit (Life Technologies). Correct insertion was confirmed by PCR. pET28-a was digested with NdeI and XhoI. Insertion of *loxA* gene from TOPO was attempted, but unsuccessful.

loxA with a His$_6$ tag was generated using Invitrogen Platinum PFX DNA Polymerase in combination with the following primers from a Custom Gateway PAO1 Clone set:

pLO151f: c acc gaa ttc atg AAT GAC TCG ATA TTC TTT TCA CCC

pLO151r: gcg ctc gag aag ctt tta tca GAT ATT GGT GCT CGC CGG GAT C

This PCR fragment was reacted with pet151d-TOPO to produce pet151/His$_6$-LoxA. The plasmid was then checked for orientation by restriction digest and the PCR fragment sequenced at the DNA Sequencing Facility of UC Berkeley to confirm the correct sequence and codon alignment.

Protein Expression and Purification.

Purification of LoxA was carried out using the N-terminal His$_6$-tag construct described above, with the parent plasmid, pet151d-TOPO (Life Technologies). The His$_6$-LoxA protein was expressed using the pet151d-TOPO plasmid in *E. coli* BL21 (DE3). The host cells were grown to 0.6 OD at 37 °C, induced by dropping the temperature to 20 °C and grown overnight (16 hr). The cells were harvested in 2L fractions at a velocity of $5,000 \times g$, then snap frozen in liquid nitrogen. The cell pellets were re-suspended in buffer A (25 mM HEPES, pH 7.5, containing 150 mM NaCl), and lysed using sonication. The cellular lysate was centrifuged at $40,000 \times g$ for 25 min, and the supernatant was loaded onto an NTA-Ni affinity column. The column was eluted with a gradient of 0–500 mM imidazole in buffer A. LoxA fractions were collected at approximately 200 mM imidazole and pooled together yielding greater than 90% purity. Protein samples were combined with glycerol to 10% (v/v) and then snap frozen under liquid nitrogen.

Protein and Metal Concentration.

LoxA was subjected to amino acid analysis to determine protein concentration. Purified protein was concentrated using a Millipore polyethersulfone 30 kD cutoff membrane in an Amicon ultrafiltration cell and analyzed at Davis Molecular Structure Facility (UCD). The same protein sample was also subjected to Bradford assay and absorbance measurement at 280 nm, allowing for calculation of the extinction coefficient. Iron content of LoxA was determined using a Finnegan inductively coupled plasma mass spectrometer (ICP-MS). An internal Co^{3+} standard and external standardized Fe solutions were used for quantitation. Enzyme concentrations were standardized to Fe content since only iron-loaded enzyme is active.

Recombinant LoxA Cleavage.

pET151/D-TOPO vector based construct adds 35 amino acids between start site and beginning of the signal-peptide-cleaved native protein. A vector TEV site was used to remove 26 of those residues, including the N-terminal His_6 tag. Recombinant His_6-TEV enzyme was used as previously described.[21,22] Kinetic properties of cleaved LoxA were compared to un-cleaved enzyme to verify that additional residues do not affect enzyme properties. Metal analysis was performed with cleaved protein as described above.

Steady-State Kinetic pH Profile.

Lipoxygenase rates were determined by following the formation of the conjugated diene product at 234 nm ($\varepsilon = 25000$ $M^{-1}cm^{-1}$). All reaction mixtures were 2 mL in volume and constantly stirred using a magnetic stir bar at room temperature (22 °C), unless otherwise described. Assays were conducted in 25 mM HEPES buffer (pH 6.5, 7.0, 7.5) containing 0.01% TX-100 with substrate concentrations ranging from 1 to 60 μM and were initiated by the addition of enzyme, as described above. Substrate concentrations were quantitatively determined by allowing the enzymatic reaction to go to completion. Kinetic data were obtained by recording initial enzymatic rates at each substrate concentration and were then fitted to the Michaelis-Menten equation using KaleidaGraph (Synergy) to determine K_{cat} and K_{cat}/K_M values.

Steady-State Kinetic Temperature Profile.

Initial rates of reaction were measured by the above methods. Temperature control of the reaction was achieved by using temperature-controlled cuvette holders. To account for temperature-induced pH differences in HEPES, buffers were equilibrated to temperatures from 22 to 45 °C and then the pH values were adjusted. Approximately 7 nM LoxA enzyme was added to initiate the reactions. Approximately 10 μM AA was used as substrate and the reactions were performed in 25 mM HEPES pH 7.0 (with no Triton X-100).

Substrate Preference.

Substrate preference was determined by comparison of the initial reaction rate by monitoring product formation on a Perkin Elmer Lambda 40 spectrophotometer at 234 nm. Approximately 7 nM LoxA enzyme was added to initiate the reaction. All substrates were at 10 μM concentration and in 25 mM HEPES pH 7.0 (with no Triton X-100).

Product Profile.

Products formed by LoxA were determined by reacting 10 μM substrate with LoxA to approximately 75% total turnover, monitored at 234 nm. Reactions were quenched with 1% glacial acetic acid and analyzed by LC-MS on a Thermo-Electron LTQ. Product separation was achieved by using a C18 HAIsil 250 × 4.6 mm analytical column (Higgins Analytical). Solution A was 99.9% acetonitrile and 0.1% acetic acid; solution B was 99.9% H_2O and 0.1% acetic acid. An isocratic gradient of 55% A and 45% B was used to purify products. The identification of LoxA products was achieved by comparing MS/MS fragments with known standards at www.lipidmaps.org. In cases where MS/MS fragmentation standards were not available, products were identified by comparing fragment masses with predicted

fragment masses with cleavage mediated by the hydroxy group near an unsaturated carbon.[23]

Product Stereochemistry.

Determining the stereochemistry of the 15-HETE produced by LoxA was achieved by Mosher ester analysis.[24] The HPLC purified LOX product (evaporated in a glass vial) was reacted with 39 equivalents of anhydrous pyridine, 100 μL of anhydrous deuterated chloroform, and 16 equivalents of either (S)-(+)-alpha-methoxy-alpha-trifluoromethylphenylacetyl chloride or (R)-(–)-alpha-methoxy-alpha-trifluoromethylphenylacetyl chloride. Samples were diluted with deuterated chloroform to a final volume of 700 μL, transferred to a 5 mm NMR tube, and then both 1D proton and 2D COSY spectra were taken (Varian 600 MHz NMR). The unmodified LOX product was also analyzed in a similar manner for comparison, and the proton assignments determined. The differences in proton chemical shifts between R and S Mosher esterified products were tabulated. Subtracting the chemical shifts between S and R spectra yields a positive or negative value, which indicates the priority of each side of the alcohol in regards to the Cahn-Ingold-Prelog convention and thus allows the determination of the absolute configuration of the secondary alcohol.[25]

Phosphoester Substrate Activity.

Affinity for phosphoester linked substrates was determined for several enzymes by comparing initial rate of phosphoester linked AA to free AA. Phosphatidylcholine with C18 in position 1 and AA in position 2 (PC-C18-AA) and Porcine Brain Phosphatidylserine (Avanti) were mixed in a 3:1 ratio and extruded into liposomes using an Avanti lipid extruder. Activity buffer consisted of 20 μM Tris pH 7.5 with 150 mM NaCl and 0.2 mM EDTA. $CaCl_2$ (4.0 mM) was added directly to the reaction mixture before enzyme addition when required. Total phospholipid concentration was approximately 20 μg/mL in activity buffer. AA reactions were performed at 10 μM substrate. Initial rates were measured as described above. Rates were normalized to enzyme concentration used in each trial.

Kinetic Isotope Effect.

The noncompetitive kinetic isotope effect on the K_{cat} $^D(K_{cat}[LA])$ and K_{cat}/K_M $^D(K_{cat}/K_M[LA])$ values was determined by comparing the steady-state kinetic results of protonated linoleic acid with that of perdeuterated linoleic acid, as previously described.[26] Kinetic measurements were performed following product formation at 234 nm, in 25 mM HEPES buffer (pH 7.0). Reactions were initiated using 8 and 160 nM LoxA for protonated and perdeuterated linoleic acid, respectively, with substrate concentrations ranging from 1 to 60 μM. Kinetic parameters were determined as described in steady-state kinetic pH profile. Kinetic isotope effect was also determined competitively as previously described.[19]

Secondary Product Profile.

LoxA products and secondary products were generated by reacting LoxA with 10 μM AA, 15-hydroperoxyeicosatetraenoic acid (15-HpETE), 5-hydroperoxyeicosatetraenoic acid (5-HpETE) as well as with their reduced hydroxyl derivatives; 15-HETE and 5-HETE. Each

reaction was 2 mL in volume and carried out in 25 mM HEPES, pH 7.0 for 30 minutes using a magnetic stir bar. Once completed, the reactions were quenched with 200 μL acetic acid and extracted three times with 1 mL of dichloromethane (DCM). The DCM was evaporated to dryness under nitrogen, and reconstituted in 100 μL methanol containing a known concentration of 13-HODE as an internal MS standard. The products were analyzed using a Thermo Scientific Velos pro mass spectrometer with an Orbitrap attached, equipped with a Phenomenex Kinetex column (c1.7 μm C18, 100 A, 150 mm × 2.1 mm) using a flow rate of 350 μL/min. Solvent A was 99.9% acetonitrile with 0.1% formic acid and solvent B was 99.9% milli Q water with 0.1% formic acid. First a gradient was used from 40% A to 45% A over 19 minutes, followed by a step to 50% A. Then a gradient was used from 50% A to 75% A over another 19 minutes. Finally, MS retention times and fragmentations were matched with standards bought from Cayman Chemical and quantified using a standard curve of each AA product. The rates of product formation found using MS were compared to rates of product formation using UV absorbance. Rates determined by UV were done using a Perkin Elmer Lambda 45 spectrophotometer by monitoring the formation of the products at their respective wavelengths. All reactions were 2 mL in volume and carried out in 25 mM HEPES buffer, pH 7.0 and continually stirred at room temperature. All substrate concentrations were 10 ± 1.0 μM.

Tryptophan Fluorescence Measurement.

The fluorescence reduction resultant of product binding previously reported for soybean LOX-1 (s15-LOX-1) was checked with LoxA.[27] Fluorescence was measured continuously as 0.5 μM LoxA was added to 2 mL of 25 mM HEPE pH 7.5. 13-HpODE (20 μM) was added to induce fluorescence decrease. s15-LOX-1 was used as a positive control.

LoxA Inhibitor Selectivity against Human LOX Inhibitors.

The one-point inhibition percentages were determined for human LOX inhibitors by following the formation of the conjugated diene product at 234 nm ($\varepsilon = 25000$ $M^{-1}cm^{-1}$) at 25 μM inhibitor concentration. All reactions were 2 mL in volume and constantly stirred using a magnetic stir bar at room temperature (22° C) with 7 nM LoxA. Reactions were carried out in 25 mM HEPES buffer (pH 7.0), 0.01% Triton X-100, and 10 μM AA. The concentration of AA was quantitatively determined by allowing the enzymatic reaction to go to completion. Confirmed hits were then screened against the human isozymes 5-LOX, 15-LOX-1, 15-LOX-2, and 12-LOX for specificity. IC_{50} values were determined by measuring percent inhibition at various inhibitor concentrations and fitted to a simple hyperbolic equation using KaleidaGraph (Synergy).

HTP LoxA Inhibitor Screen.

The Library of Pharmacologically Active Compounds (LOPAC)[28] were also screened in qHTS format[29] for potential selective LoxA inhibitors using a Xylenol orange high throughput screening (HTS) assay previously developed by our lab. Compounds flagged as inhibitors in the HTS screen were retested in the manual cuvette assay against LoxA for potency.

Prior to screening, enzyme and substrate concentration, in addition to reaction time were optimized with regard to enzyme kinetics, quantity of reagents, and signal window.[30,31] Briefly, 3 μL of enzyme (approximately 20 nM LoxA, final concentration) or buffer (no-enzyme control) were dispensed into 1,536-well Greiner black clear-bottom assay plates using a BioRAPTR Flying Reagent Dispenser (Beckman Coulter, Fullerton, CA). Compounds and controls (broad spectrum LOX inhibitor, nordihydroguaiaretic acid (NDGA), concentration ranging from 3.4 mM to 0.208 μM) were transferred (23 nL or 46 nL) via Kalypsys PinTool, equipped with 1536-pin array, to yield final library compound concentrations ranging from 114 μM to 0.73 nM.[32] The plate was covered and incubated for 15 min at room temperature, followed by an addition of a 1 μL aliquot of substrate solution (40 μM arachidonic acid final concentration; $K_m = 10$ μM) to start the reaction, for a final assay volume of 4 μL. The reaction was stopped after 15 minutes (~90% conversion, data not shown) by the addition of 4 μL FeXO solution (final concentrations of 200 μM XO and 300 μM ferrous ammonium sulfate in 50 mM sulfuric acid). After a short spin (1000 rpm, 15 sec), the assay plate was incubated at room temperature for 30 minutes and the absorbances at 405 and 573 nm were collected using a ViewLux high throughput CCD imager (Perkin-Elmer, Waltham, MA) using standard absorbance protocol settings. During dispense, enzyme and substrate bottles were kept on ice to minimize degradation.

Percent inhibition was computed from the median values of the catalyzed, or neutral control, and the uncatalyzed, or 100% inhibited control, respectively, and plate-based data corrections were applied to filter out background noise.[33] Average Z′ was 0.59 across six 1,536-well assay plates, with a signal to background of 1.8. The intraplate control compound NDGA performed extremely well, with an IC_{50} value of 23 μM and MSR[34] of 2.1.

The screen and subsequent cheminformatics analysis yielded 94 potential hits, of which 22 compounds were selected using a cheminformatics analysis process previously described.[29] Compound were subsequently retested using the manual cuvette assay.

LoxA Antibody Purification.

Polyclonal rabbit antibody was raised to purified recombinant LoxA protein by Pocono Rabbit Farm & Laboratory. Antibody was purified from whole blood by affinity for the purified recombinant LoxA protein, immobilized using a Pierce Aminolonk immobilization kit. Coupling and antibody purification was performed following manufacturers recommendation. Briefly, 3 mL of 2 mg/mL recombinant protein in pH 7.2 phosphate buffer was rocked in column overnight at 20° C. Reaction was quenched and column was washed and stored at 4 °C. 4 mL rabbit serum was loaded on column and washed with 7 mL PBS, 1 mL 1 M NaCl, 7 mL PBS and eluted with 6 mL glycine. 1.5 mL fractions were collected and subjected to Bradford protein analysis. Eluted fractions with >0.05 mg/mL protein were combined and 10% glycerol was added. Pooled AB aliquots were frozen in liquid nitrogen and stored at −80 °C.

P. aeruginosa Mutant Strain Growth and LoxA Production Analysis.

LoxA production was determined using immunoprecipitation and western blot analysis. 50 mL liquid cultures of wild type (PAO1), *loxA*::Tn (*loxA* transposon mutant to disrupt *loxA*

gene expression), *wspF* mutant (*wspF* gene deletion strain), *loxA* overexpression (both induced and non-induced) strains were grown overnight in Luria broth at 37 °C, shaking at 225 rpm. To promote biofilm formation wild-type, *loxA*::Tn, and *wspF* mutant strains were also grown at minimal agitation (30 rpm) with a stir bar to facilitate biofilm adhesion. LoxA overexpression was induced by adding 0.5% arabinose 4 hr before harvesting. Cultures were pelleted at $10,000 \times G$, 4 °C, resuspended in lysis buffer and sonicated. Cellular debris was removed by centrifuging at $15,000 \times G$. Immunoprecipitation was performed using Protein A beads (Santa Cruz Biotech) following manufacturer instructions. Briefly, Bradford assay was performed and 2 mg total cellular protein was combined with 20 μL bead slurry. After incubation, 2 μL of crude LoxA antibody sera was added. Beads were incubated and washed. PAGE was performed using Life Technologies NuPAGE 4–12% Bis-Tris gels with MOPS running buffer. A western blot was performed using purified LoxA polyclonal antibody as the primary and Sigma Aldrich goat anti-rabbit IgG HRP as the secondary. Bands were visualized using Pierce ECL western blotting substrate. Bands were detected and quantified using a BioRad ChemiDoc XRS System. Loading control was performed to verify that Bradford normalization of immunoprecipitation samples was accurate. For this, a western blot was performed with normalized samples using Neoclone RpoA antibody as the primary and Sigma Aldrich goat anti mouse HRP antibody as the secondary. Analysis was performed as above.

Bacterial Cloning.

To complement the *loxA* defect in the PW3111 transposon mutant, the *loxA* gene was fused to a constitutive promoter and inserted at a neutral site on the genome. The *nptII* promoter was used for constitutive expression and amplified from pMQ118[35] by PCR using forward primer 5'-GAGCTCCGCTGCCGCAAGCACTCAG-3' and reverse primer 5'-ACTAGTTCCTCATCCTGTCTCTTGATCAGATCTTG-3'. The P*nptII* fragment was inserted into pUC18-mini-Tn7T-Gm[36] by digestion with SacI and SpeI (NEB) followed by ligation with T4 DNA ligase (NEB) to create pUC18-mini-Tn7T-Gm-P *nptII*. Ligations were transformed into *E. coli* DH5α and transformants were selected on LB agar containing 100 μg/mL ampicillin. The *loxA* gene was amplified from *P. aeruginosa* strain MPAO1 genomic DNA by PCR using forward primer 5'-CCCGGGATGAAACGCAGGAGTGTGCTCTTG-3' and reverse primer 5'-GGTACCTCAGATATTGGTGCTCGCCGG-3'. The *loxA* fragment was inserted into pUC18-mini-Tn7T-Gm-P*nptII* by digestion with XmaI and KpnI and ligation with T4 DNA ligase to create pUC18-mini-Tn7T-Gm-P*nptII-loxA*. Ligations were transformed into *E. coli* DH5α and transformants were selected on LB agar containing 100 μg/mL ampicillin. Correct construction of the pUC18-mini-Tn7T-Gm-P*nptII-loxA* was confirmed by Sanger sequencing with forward primer 5'-GAACTTCAGAGCGCTTTTGAAGCTAATTC-3' and reverse primer 5'-GGGAACTGGGTGTAGCGTCGTAAGC-3'. The pUC18-mini-Tn7T-Gm-P*nptII-loxA* plasmid was inserted at the *att*Tn7 site downstream of the *glmS* gene in the PW3111 transposon mutant strain by co-transformation with a pTNS3 helper plasmid constitutively producing the Tn7 transposase.[36] Colonies were isolated on LB agar plates containing 50 μg/mL gentamycin and 50 μg/mL tetracycline to ensure retention of the transposon as well as insertion of the complement plasmid. Insertion of the complement plasmid at the *att*Tn7 site was confirmed by PCR using forward primer 5'-

CACAGCATAACTGGACTGATTTC-3' and reverse primer 5'-GCACATCGGCGACGTGCTCTC-3'.

Airway Epithelial Cell Culture.

Airway epithelial cells were cultured as previously described.[37] In brief, the human bronchial epithelial cells (16HBE cell line) were seeded at 7.4×10^4 cells per 6.5 mm transwell filter (Corning), before polarization at air-liquid interface for seven days prior to the start of the biotic biofilm/attachment assay.

Biotic Biofilm/Attachment Assay.

To examine *P. aeruginosa* biofilm growth in association with airway epithelial cells, we followed previously published methods.[37] Briefly, the airway epithelial cells were rinsed in minimal essential media (MEM) and the washed bacteria were applied at an MOI between 25 and 30. After one hour, the apical media was removed and replaced with the MEM + 0.4% L-arginine, and the biofilms were allowed to grow for an additional five hours at 37 °C. At the end of the five hour incubation, the cells were washed once with MEM and biofilms were removed with 0.1% Triton-X 100 and serially diluted to determine the colony forming units (CFU). For the attachment assay, the wash steps and determination of colony forming units immediately followed the one-hour incubation on airway epithelial cells. For experiments with recombinant LoxA protein, 1ug protein was added directly to the apical surface of the epithelial cells in MEM media.

Abiotic Biofilm Assay.

Microtiter abiotic biofilm assays were performed, as previously published.[38] Bacterial cultures were prepared as described above. The overnight cultures were then diluted 1:30 in minimal essential media and plated in a 96-well dish. The bacteria were grown for 24 hours without agitation at 37 °C. Following incubation, the liquid media was removed, and the biofilm were washed and stained with 41% crystal violet solution in water. Biofilm growth was quantified by reading absorbance in a plate reader at 550 nm.

Results and Discussion

Sequence Alignment.

The sequence of *P. aeruginosa* LoxA was compared to s15-LOX-1 and human 5-LOX, 12-LOX, 15-LOX, and 15-LOX-2 using the alignment program Clustal Omega, available at http://www.clustal.org/omega.[39] Alignment statistics are shown in Table 1. Interestingly, the protein with greatest identity and similarity is 5-LOX. LoxA has an asparagine as the fifth coordination ligand (N540), similar to s15-LOX-1, 12-LOX and 5-LOX. However, the highest alignment score goes to 15-LOX-2. Pairwise alignment scores from Clustal Omega are calculated by taking the number of identities between the two sequences, divided by the length of the alignment, and presenting this number as a percentage. The alignment score (and similarity) for s15-LOX-1 is better than 15-LOX-1, but this does not take into account the large sequence gaps that appear in the human and *Pseudomonas* proteins when aligned with the significantly larger plant enzyme.

Protein Expression and Purification Yield.

The construction of the LoxA plasmid was difficult to achieve by standard methods, therefore, Life Technologies Champion pET151 directional TOPO expression kit was used. The final recombinant construct of LoxA used in this study contains an N-terminal His_6 tag, followed by 29 residues from the TOPO expression vector that are not present in the wild type LoxA gene (Figure 1). This construct lacks the 19 amino acid predicted signal peptide region, which is present on the N-terminus of the bacterial enzyme, but presumably cleaved before the protein is excreted. The gene in the plasmid was successfully sequenced, however, there was difference from the reported sequence, with Gly 324 being replaced by Asp in our vector. We considered this a normal variant of the gene because the mutation was determined to be in the original Gateway PAO1 Clone set by sequencing. In addition, it is not a conserved residue in an essential portion of the protein, so we did not change the residue.

Recombinant LoxA was expressed in *E. coli* on 4 L scale at 22 °C and purified with Probond Ni resin, yielding 48 mg of >90% pure protein based on SDS PAGE gel (data not shown). Pure protein had an approximate molecular weight (MW) of 76 kD based on gel MW markers. The concentration of LoxA in a sample of pure protein was determined by amino acid analysis and used to establish an extinction coefficient of 169000 $M^{-1}cm^{-1}$ at 280 nm. Thus, 1.0 absorbance unit equates to 2.20 mg/mL of LoxA protein. ICPMS was performed and the purified recombinant LoxA was determined to be 67% metalated. This enzyme concentration was subsequently used to determine the K_{cat} and K_m of 15p-LOX. To verify that the additional 26 amino acids added by the expression vector has no effect on enzymatic activity, the enzyme was cleaved with TEV and kinetics were compared at pH 7.0 in the presence and absence of TX-100. Metal content was also compared by ICPMS using cleaved and uncleaved enzyme. No difference in activity or metal content were observed (data not shown).

Enzyme Kinetics, pH and Temperature Dependence.

The kinetic parameters, K_{cat} and K_{cat}/K_m were determined as a function of pH using AA as the substrate (Table 2). The greatest kinetic efficiency was observed at pH 6.5. Activity decreased quickly below pH 6.5, as described previously by activity measurements in culture media.[14] This may be related to decreasing substrate solubility at low pH. The enzymatic activity above pH 7.5 decreases rapidly to almost no observable turnover. Due to the low solubility of the substrate at pH 6.5, all subsequent kinetic measurements in this study were performed at pH 7.0 to balance enzyme activity with substrate solubility. Interestingly, this is shifted slightly from previous observations using KH_2PO_4 buffer and LA substrate.[18] In contrast, human LOX enzymes have maximal activity above pH 7.0, while s15-LOX-1 is most active at pH 9.0. The structural basis for the low pH preference of LoxA is as yet unclear. However, it is interesting to note that the pH of the extra-cellular fluid within the lung is close to pH 7, and becomes lower in patients with cystic fibrosis, where chronic *P. aeruginosa* infections are common.[40]

Kinetic rate measurements for selected 15-LOX isozymes are compared in Table 3. The enzymatic efficiency of LoxA at pH 6.5 far exceeds that of its human homologues,[41] and is

similar to the soybean 15-LOX enzyme (s15-LOX-1).[42] The 5 endogenous ligands to the LoxA iron site consist of three histidines (His 353, His 358 and His 536), the C-terminal isoleucine carboxylate and Asn 540, similar to the coordination environments of 5-LOX, 12-LOX and s15-LOX-1. The presence of the asparagine at the 5th coordination site can help to rationalize the high kinetic rate of this enzyme, as the weak Asn ligand has been shown to increase kinetic efficiency by increasing the reduction potential of the iron, thus making the abstraction of the hydrogen more facile.[43]

The enzymatic activity of LoxA as a function of temperature was determined. Little variation was observed in the enzymatic activity over the range of 22 °C to 35 °C, however, activity decreased significantly above 35 °C (data not shown). This data is in agreement with previous studies indicating an optimum temperature of 25 °C,[44] and suggests that an *in vivo* activity for LoxA would be more likely in the nasal passages or the skin (with temperatures ranging from 25–33 °C), as compared to infections of the lower respiratory tract.

Substrate Preference and Product Profile.

The substrate preference and product profile differences of the human 15-LOX isozymes may be the basis of their distinct biological activities.[45,46] To investigate the ability of LoxA to produce biologically relevant LOX products, the enzyme activity with a range of possible LOX substrates was determined. Substrates were ranked by initial rate observed at 10 μM using UV absorbance detection (Table 4). Products produced from each substrate were determined by HPLC-MS/MS and shown ranked by percent of total product peak area. The LoxA reaction with AA produces predominantly 15-HETE as previously determined.[14] The most reactive substrates tend to produce predominantly a single product while slower substrates generally produce higher percentages of minor products. Dihomo-gamma-linolenic acid (DGLA) is a notable exception to this trend, with a low catalytic efficiency but only one observed product. Reaction with LA produces predominantly 13-HODE as previously established.[18] Similar to 15-LOX-2, LoxA prefers AA substrate over LA and does not produce significant 12-HETE product.[47] Interestingly, a recent study observed a reduction in 15-LOX-2 expression in cystic fibrosis (CF) patients, which was correlated with lower levels of the inflammatory resolution mediator, lipoxin A_4.[48] Considering *P. aeruginosa* is an important cause of chronic infection for CF patients, the interplay between LoxA product generation and the unique conditions of the CF lung require further investigation.

Product Stereochemistry.

To verify that LoxA products will have the same biological effects as those generated from the human 15-LOX enzymes, the stereochemistry of 15-HETE generated from the *P. aeruginosa* enzyme was determined. Mosher analysis was performed on 15-HETE generated from enzymatic reaction with LoxA, as previously described.[24,25] The change in chemical shift for each proton of the R-mosher reacted product can be subtracted from that of the *S*-mosher reacted product, and the resulting shift difference determines the stereochemistry of the original product (Figure 2). Chemical shift values indicate that the 15-(S)-HETE product is generated by LoxA, which is similar to human 15-LOX enzymes. This result is in

agreement with the chiral HPLC experiment performed previously using 13-HPOD generated by LoxA.[18]

Phosphoester Substrate Activity.

LoxA has been speculated to use phosphoester-linked substrate natively.[49] To test this hypothesis, the ability of LoxA to react with PC-AA was examined (Table 5). For comparison, the human enzymes 15-LOX-1, 15-LOX-2 and 12-LOX were also assayed. Enzymes were compared by normalizing max rate of PC-AA catalysis to the initial rate of AA turnover under similar conditions. Thus, enzymes are ranked by activity with PC-AA as a percentage of that enzyme's AA rate. Reactions were run in the presence and absence of calcium as it has been shown to aid in membrane binding.[50] Of the enzymes tested, LoxA had the slowest relative rate under both calcium-added and no-calcium conditions. The ability of 15-LOX-1 to oxidize phospoester-linked substrates is similar to that of LoxA in the absence of calcium, but significantly higher with calcium present. 15-LOX-2 is kinetically the slowest enzyme tested with AA, but its PC-AA is highest relative to its rate with AA. LoxA and 15-LOX-2 both show a small increase in PC-AA reaction rate when calcium is added. 12-LOX lies in between the human 15-LOX isozymes with respect to reaction rate with PC-AA but interestingly is the only enzyme whose peroxidating ability is unaffected by the addition of calcium. Although LoxA is faster than the human 15-LOX enzymes with free fatty acid substrates, the absolute rate of peroxidation of the phosphoester-linked substrate by the bacterial enzyme is comparable to human LOX rates. It should be noted that the pH of this assay (pH 7.5) is not optimal for LoxA, and thus its rate is not significantly greater than human 15-LOX-1. LoxA was also assayed at pH 7.0, but no significant difference in phospholipid peroxidating ability was observed.

Kinetic Isotope Effect.

To verify that hydrogen atom abstraction is rate limiting, as it the case with other LOX enzymes,[19,26] the noncompetitive kinetic isotope effect (KIE) was determined for LoxA with LA. The KIE for K_{cat} was 32 +/− 6 and for K_{cat}/K_m the KIE is 450 +/− 70 (Table 6). High error in the K_{cat}/K_m KIE is due to the large error in K_m, most likely due to the poor solubility of the substrate above 30 μM at pH 7. The competitive method for determination of the KIE was also performed, however the magnitude of the KIE made detection of the deuterated product difficult via HPLC, adding to its error. The K_{cat}/K_m KIE from the competitive method was estimated at 120 +/− 70, consistent with the large K_{cat}/K_m KIE, seen with the noncompetitive method. The large KIE is consistent with other LOX isozymes and indicates that hydrogen abstraction proceeds through a tunneling mechanism and is a rate-limiting step in the reaction.[19]

Secondary Product Profile.

LoxA secondary product profiling was performed to identify any products made by LoxA when reacted with different HpETE and HETEs. 15-HpETE, 15-HETE, 5-HpETE and 5-HETE were chosen as substrates due to their reaction products (5,15-diHpETE and 5,15-diHETE) being potential precursors to the formation of lipoxin (LXB$_4$). Rates of these reactions were compared to the rates with AA. The K_{cat} for LoxA with its preferred substrate AA was found to be 3.13 sec^{-1} (moles product/sec/moles enz). Relative to the K_{cat}

with AA, LoxA reacted 10,000 times slower with 15-HpETE and 100,000 times slower with 15-HETE. The K_{cat} for 5-HpETE and 5-HETE was 100,000 times slower. (Table 7) The small production of 5,15-diHpETE and 5,15-diHETE was confirmed with mass spectrometry. The slow rate of formation of these diHpETE and diHETEs by LoxA brings into question the relevance of this reaction. However, it should be noted that in epithelial lung tissue, human 15–1 lipoxygenase is expressed at high levels[51,52] and has been shown to convert these diHpETE and diHETE products into LXB4,[53,54] so LoxA could have a similar effect if expressed at high levels.

Tryptophan Fluorescence Measurement.

s15-LOX-1 exhibits a unique fluorescence signal which can be quenched with addition of 13-HpODE.[27] To determine if LoxA also has this property, the fluorescence of LoxA was measured with the addition of an excess of 13-HpODE. No decrease in fluorescence was observed. The fluorescence change of s15-LOX-1 arises from decreases in tryptophan fluorescence due to tryptophan residue in the vicinity of the s15-LOX-1 active site. Only tryptophans 480, 618, 624 and 648 of s15-LOX-1 align with tryptophans in the LoxA sequence.

LOX Inhibitor Selectivity.

In order to determine the feasibility of specific inhibition of LoxA in a biologically relevant context, the cross reactivity of several high potency, high specificity human lipoxygenase inhibitors for LoxA were assayed. IC_{50} values for these compounds against LoxA are shown in Figure 3. Inhibition of LoxA was determined via one point screen, as described previously.[55] The 15-LOX-1 active compound chosen was a recently reported highly specific, nanomolar potent 15-LOX-1 inhibitor.[56] The potency difference observed when assayed against LoxA was approximately 2000-fold. A selective 15-LOX-2 inhibitor was also assayed and showed the smallest difference in potency from its selective enzyme of all inhibitors tested.[57] However, this may be due to the relatively low potency of this inhibitor compared to the selective inhibitors for other isozymes. The chosen 12-LOX compound was also a recently reported high specificity inhibitor.[58] This compound had no effect on LoxA. The 5-LOX specific inhibitor chosen showed a potency decrease of 100-fold. It is interesting that 5-LOX and 15-LOX-2 inhibitors have the smallest potency difference since they also have the highest degree of sequence similarity to LoxA based on alignment data. The nonspecific reductive inhibitor NDGA was also assayed, and exhibited an IC_{50} value comparable to the values obtained against the human enzymes.[59]

HTP LoxA Inhibitor Screen.

To complement our search for LoxA-specific inhibitors, we screened the Library of Pharmacologically Active Compounds (LOPAC) using a high throughput screening assay developed earlier by our lab.[60] Nine of the top compounds that showed the largest inhibition in the screen were further investigated for selectivity to LoxA versus the other human isozymes using single-point screens (Table 8). To confirm their potency to LoxA, IC_{50} studies were performed (Table 9). The IC_{50} studies validated that these compounds were potent towards LoxA, with IC_{50} values ranging from ~4 to ~16 μM. The most potent compound NCGC00015424 had an IC_{50} value of 4.1 ± 1.4 μM with selectivity towards

LoxA over 12-LOX and 15-LOX-2 and not the other human isozymes. The second and third potent compounds, NCGC00018102 and NCG00015802 had IC_{50} values of 4.5 ± 0.4 μM and 5.8 ± 1.4 μM respectively, with selectivity towards LoxA over 12-LOX, 15-LOX-1, and 15-LOX-2. See tables 8 and 9 for IC_{50} values and selectivity data for the less potent compounds.

LoxA *in vivo* Production.

To probe the production level of LoxA in *P. aeruginosa* during varying growth conditions, western blots were performed. Previous experiments showed that mRNA was increased during abiotic biofilm growth.[60] To test whether this corresponds to a significant protein abundance increase during biofilm growth, a western blot for LoxA was performed with *P. aeruginosa* cultures grown in planktonic and biofilm growth conditions (Figure 4). Under planktonic growth conditions, wild type PAO1 has no detectable production of LoxA. Using biofilm growth conditions, wild type bacteria displays a low level of detectable LoxA protein. Using a *wspF* deletion mutant strain, which forms biofilms more quickly and to a greater extent than wild type PAO1,[61] we observed a low level of LoxA production in planktonic culture, and dramatically increased protein abundance in biofilm conditions for the mutant (Figure 4). In agreement with previously published mRNA data, these data indicate that conditions that favor biofilm growth correspond to higher levels of LoxA production.

Since LoxA production was increased during biofilm growth, we next investigated if LoxA had a role in *P. aeruginosa* biofilm growth. To test this hypothesis, we first examined biofilm growth of wild-type *P. aeruginosa* and a *loxA* transposon mutant in a microtiter dish biofilm assay. We observed no change in biofilm growth of *P. aeruginosa* with the *loxA* mutant (Figure 5). Moreover, in an abiotic setting of biofilm growth, addition of LoxA protein to complement the mutant or even addition to wild-type bacteria did not alter biofilm growth (Figure 5).

Due to the previously observed interactions of *P. aeruginosa* with host-derived lipids, we also examined if LoxA mediates *P. aeruginosa* biofilm growth in association with the host. To test this hypothesis, we used a unique model system where *P. aeruginosa* biofilms are cultured on the surface of airway epithelial cells, mimicking a colonizing infection in the host. Bacterial biofilms grown in the setting of the host airway epithelium quickly transition to a biofilm mode of growth, as measured by gene expression and acquisition of incredible antibiotic resistance.[62] Using this biotic biofilm model, we observed a decrease in bacterial biofilm growth with the *loxA* transposon mutant, as compared to wild-type *P. aeruginosa* (Figure 6A). This decrease could be complemented by expression *loxA* in the transposon mutant bacteria (Figure 6A) or by delivering recombinant LoxA protein (Figure 6B). We confirmed that the reduction in biotic biofilm growth in the *loxA* mutant bacteria was not due to altered attachment to the airway epithelial cells (Figure 6C). Taken together, these results suggest that LoxA is required for *P. aeruginosa* biofilm growth in association with host tissue, but not in an abiotic setting. Future studies to determine the mechanism by which LoxA alters lipid signaling to promote biofilm formation in the host are of great interest.

Conclusions.

The current experimental results indicate that LoxA is a highly active enzyme capable of efficiently catalyzing the peroxidation of a broad range of free fatty acid substrates with high positional specificity. Its mechanism is through a hydrogen-atom abstraction and yet LoxA is a poor catalyst against phosphoester-FAs and HETEs, suggesting that LoxA may not be involved in membrane decomposition or lipoxin signaling. In addition, production of LoxA is increased in biofilm growth, and while LoxA is not required for abiotic biofilm growth, it does appear to contribute to biofilm growth in association with host tissue. We are currently utilizing the newly discovered LoxA selective inhibitors to determine if inhibition of LoxA will impact *P. aeruginosa* biofilm growth on host cells, and ultimately serve as a novel therapeutic approach to combat chronic *P. aeruginosa* infections.

Acknowledgements.

Abbreviations:

AA	arachidonic acid
5,12-DiHETE	5,12-dihydroxy-6E,8E,10E,14Z-eicosatetraenoic acid
5(S)-HETE	5(S)-hydroxy-6E,8Z,11Z,14Z-eicosatetraenoic acid
5(S)-HpETE	5(S)-hydroperoxy-6E,8Z,11Z,14Z-eicosatetraenoic acid
13(S)-HpODE	13(S)-hydroperoxy-9Z,11E-octadecadienoic acid
k_{cat}	the rate constant for product release
k_{cat}/K_m	the rate constant for substrate capture
LOX	lipoxygenase
5-LOX	human 5-lipoxygenase
12-LOX	human platelet 12-lipoxygenase
15-LOX-1	human reticulocyte 15-lipoxygenase-1
15-LOX-2	human epithelial 15-lipoxygenase-2
soybean LOX-1	soybean lipoxygenase 1
LTA$_4$	leukotriene A$_4$
LTB$_4$	leukotriene B$_4$

LXA$_4$	lipoxin A$_4$
LXB$_4$	lipoxin B$_4$
PLAT	polycystin-1/lipoxygenase/alpha-toxin
PMNL	polymorphonuclear leukocyte
PUFA	polyunsaturated fatty acid
RvD1	resolvin D1
RvE1	resolvin E1
MEM	Minimal essential media
MOI	multiplicity of infection
CFU	colony forming units

References

(1). Inweregbu K, Dave J, and Pittard A (2005) Nosocomial infections. Contin. Educ. Anaesth. Crit. Care Pain 5, 14–17.

(2). George AM, Jones PM, and Middleton PG (2009) Cystic fibrosis infections: treatment strategies and prospects. FEMS Microbiol. Lett 300, 153–164. [PubMed: 19674113]

(3). Donaldson SH, and Boucher RC (2003) Update on pathogenesis of cystic fibrosis lung disease. Curr. Opin. Pulm. Med 9, 486–491. [PubMed: 14534400]

(4). Filkins LM, Hampton TH, Gifford AH, Gross MJ, Hogan DA, Sogin ML, Morrison HG, Paster BJ, and O'Toole GA (2012) Prevalence of Streptococci and Increased Polymicrobial Diversity Associated with Cystic Fibrosis Patient Stability. J. Bacteriol 194, 4709–4717. [PubMed: 22753064]

(5). Robertson DM, Petroll WM, Jester JV, and Cavanagh HD (2007) Current concepts: Contact lens related Pseudomonas keratitis. Contact Lens Anterior Eye 30, 94–107. [PubMed: 17084658]

(6). Costerton JW, Stewart PS, and Greenberg EP (1999) Bacterial biofilms_a common cause of persistent infections.pdf. Science 284, 1318–1322. [PubMed: 10334980]

(7). Mah T-FC, and O'Toole GA (2001) Mechanisms of biofilm resistance to antimicrobial agents. Trends Microbiol. 9, 34–39. [PubMed: 11166241]

(8). Anderson GG, Moreau-Marquis S, Stanton BA, and O'Toole GA (2008) In Vitro Analysis of Tobramycin-Treated Pseudomonas aeruginosa Biofilms on Cystic Fibrosis-Derived Airway Epithelial Cells. Infect. Immun 76, 1423–1433. [PubMed: 18212077]

(9). Hubeau C, Lorenzato M, Couetil JP, Hubert D, Dusser D, Puchelle E, and Gaillard D (2001) Quantitative analysis of inflammatory cells infiltrating the cystic fibrosis airway mucosa. Clin. Exp. Immunol 124, 69–76. [PubMed: 11359444]

(10). Bonfield TL, Panuska JR, Konstan MW, Hilliard KA, Hilliard JB, Ghnaim H, and Berger M (1995) Inflammatory cytokines in cystic fibrosis lungs. Am. J. Respir. Crit. Care Med 152, 2111–2118. [PubMed: 8520783]

(11). Dean TP, Dai Y, Shute JK, Church MK, and Warner JO (1993) Interleukin-8 concentrations are elevated in bronchoalveolar lavage, sputum, and sera of children with cystic fibrosis. Pediatr. Res 34, 159–161. [PubMed: 8233718]

(12). Noah TL, Black HR, Cheng P-W, Wood RE, and Leigh MW (1997) Nasal and bronchoalveolar lavage fluid cytokines in early cystic fibrosis. J. Infect. Dis 175, 638–647. [PubMed: 9041336]

(13). Schuster A, Haarmann A, and Wahn V (1995) Cytokines in neutrophil-dominated airway inflammation in patients with cystic fibrosis. Eur. Arch. Otorhinolaryngol 252, S59–S60. [PubMed: 7537567]

(14). Vance RE, Hong S, Gronert K, Serhan CN, and Mekalanos JJ (2004) The opportunistic pathogen Pseudomonas aeruginosa carries a secretable arachidonate 15-lipoxygenase. Proc. Natl. Acad. Sci. U. S. A 101, 2135–2139. [PubMed: 14766977]

(15). Starkey M, Hickman JH, Ma L, Zhang N, De Long S, Hinz A, Palacios S, Manoil C, Kirisits MJ, Starner TD, Wozniak DJ, Harwood CS, and Parsek MR (2009) Pseudomonas aeruginosa Rugose Small-Colony Variants Have Adaptations That Likely Promote Persistence in the Cystic Fibrosis Lung. J. Bacteriol 191, 3492–3503. [PubMed: 19329647]

(16). Kirschnek S, and Gulbins E (2006) Phospholipase A2 Functions in Pseudomonas aeruginosa-Induced Apoptosis. Infect. Immun 74, 850–860. [PubMed: 16428727]

(17). Bannenberg GL, Aliberti J, Hong S, Sher A, and Serhan C (2004) Exogenous Pathogen and Plant 15-Lipoxygenase Initiate Endogenous Lipoxin A 4 Biosynthesis. J. Exp. Med 199, 515–523. [PubMed: 14970178]

(18). Lu X, Zhang J, Liu S, Zhang D, Xu Z, Wu J, Li J, Du G, and Chen J (2013) Overproduction, purification, and characterization of extracellular lipoxygenase of Pseudomonas aeruginosa in Escherichia coli. Appl. Microbiol. Biotechnol 97, 5793–5800. [PubMed: 23064455]

(19). Lewis ER, Johansen E, and Holman TR (1999) Large Competitive Kinetic Isotope Effects in Human 15-Lipoxygenase Catalysis Measured by a Novel HPLC Method. J. Am. Chem. Soc 121, 1395–1396.

(20). Jacobs MA, Alwood A, Thaipisuttikul I, Spencer D, Haugen E, Ernst S, Will O, Kaul R, Raymond C, Levy R, and others. (2003) Comprehensive transposon mutant library of Pseudomonas aeruginosa. Proc. Natl. Acad. Sci 100, 14339–14344. [PubMed: 14617778]

(21). Joshi N, Hoobler EK, Perry S, Diaz G, Fox B, and Holman TR (2013) Kinetic and Structural Investigations into the Allosteric and pH Effect on the Substrate Specificity of Human Epithelial 15-Lipoxygenase-2. Biochemistry (Mosc.) 52, 8026–8035.

(22). Blommel PG, and Fox BG (2007) A combined approach to improving large-scale production of tobacco etch virus protease. Protein Expr. Purif 55, 53–68. [PubMed: 17543538]

(23). Murphy RC, Barkley RM, Zemski Berry K, Hankin J, Harrison K, Johnson C, Krank J, McAnoy A, Uhlson C, and Zarini S (2005) Electrospray ionization and tandem mass spectrometry of eicosanoids. Anal. Biochem 346, 1–42. [PubMed: 15961057]

(24). Hoye TR, Jeffrey CS, and Shao F (2007) Mosher ester analysis for the determination of absolute configuration of stereogenic (chiral) carbinol carbons. Nat. Protoc 2, 2451–2458. [PubMed: 17947986]

(25). Ikei KN, Yeung J, Apopa PL, Ceja J, Vesci J, Holman TR, and Holinstat M (2012) Investigations of human platelet-type 12-lipoxygenase: role of lipoxygenase products in platelet activation. J. Lipid Res 53, 2546–2559. [PubMed: 22984144]

(26). Glickman MH, and Klinman JP (1995) Nature of rate-limiting steps in the soybean lipoxygenase-1 reaction. Biochemistry (Mosc.) 34, 14077–14092.

(27). Ruddat VC, Mogul R, Chorny I, Chen C, Perrin N, Whitman S, Kenyon V, Jacobson MP, Bernasconi CF, and Holman TR (2004) Tryptophan 500 and Arginine 707 Define Product and Substrate Active Site Binding in Soybean Lipoxygenase-1 †. Biochemistry (Mosc.) 43, 13063–13071.

(28). Library of Pharmacologically Active Compounds.pdf.

(29). Inglese J, Auld DS, Jadhav A, Johnson RL, Simeonov A, Yasgar A, Zheng W, and Austin CP (2006) Quantitative high-throughput screening: a titration-based approach that efficiently identifies biological activities in large chemical libraries. Proc. Natl. Acad. Sci 103, 11473–11478. [PubMed: 16864780]

(30). Geeganage S, Kahl SD, Montrose C, Sittampalam S, Smith MC, and Weidner JR (2012) Basics of Enzymatic Assays for HTS.pdf.

(31). Jameson JB, Kantz A, Schultz L, Kalyanaraman C, Jacobson MP, Maloney DJ, Jadhav A, Simeonov A, and Holman TR (2014) A High Throughput Screen Identifies Potent and Selective Inhibitors to Human Epithelial 15-Lipoxygenase-2. PLoS ONE (Jung M, Ed.) 9, e104094. [PubMed: 25111178]

(32). Yasgar A (2008) Compound Management for Quantitative High-Throughput Screening. J. Assoc. Lab. Autom 13, 79–89.

(33). Southall NT, Jadhav A, Huang R, Nguyen T, and Wang Y (2009) Enabling the Large-Scale Analysis of Quantitative High-Throughput Screening Data, in Handbook of Drug Screening 2nd ed, pp 442–464.

(34). Haas JV, Eastwood BJ, Iversen PW, and Weidner JR (2013) Minimum Significant Ratio–A Statistic to Asses Assay Variability.

(35). Shanks RMQ, Kadouri DE, MacEachran DP, and O'Toole GA (2009) New yeast recombineering tools for bacteria. Plasmid 62, 88–97. [PubMed: 19477196]

(36). Choi K-H, and Schweizer HP (2006) mini-Tn7 insertion in bacteria with single attTn7 sites: example Pseudomonas aeruginosa. Nat. Protoc 1, 153–161. [PubMed: 17406227]

(37). Zemke AC, Shiva S, Burns JL, Moskowitz SM, Pilewski JM, Gladwin MT, and Bomberger JM (2014) Nitrite modulates bacterial antibiotic susceptibility and biofilm formation in association with airway epithelial cells. Free Radic. Biol. Med 77, 307–316. [PubMed: 25229185]

(38). Hendricks MR, Lashua LP, Fischer DK, Flitter BA, Eichinger KM, Durbin JE, Sarkar SN, Coyne CB, Empey KM, and Bomberger JM (2016) Respiratory syncytial virus infection enhances Pseudomonas aeruginosa biofilm growth through dysregulation of nutritional immunity. Proc. Natl. Acad. Sci 113, 1642–1647. [PubMed: 26729873]

(39). Sievers F, Wilm A, Dineen D, Gibson TJ, Karplus K, Li W, Lopez R, McWilliam H, Remmert M, Soding J, Thompson JD, and Higgins DG (2014) Fast, scalable generation of high-quality protein multiple sequence alignments using Clustal Omega. Mol. Syst. Biol 7, 539–539.

(40). Song Y (2005) Hyperacidity of secreted fluid from submucosal glands in early cystic fibrosis. AJP Cell Physiol. 290, C741–C749.

(41). Wecksler AT, Kenyon V, Deschamps JD, and Holman TR (2008) Substrate Specificity Changes for Human Reticulocyte and Epithelial 15-Lipoxygenases Reveal Allosteric Product Regulation [†]. Biochemistry (Mosc.) 47, 7364–7375.

(42). Schenk G, Neidig ML, Zhou J, Holman TR, and Solomon EI (2003) Spectroscopic Characterization of Soybean Lipoxygenase-1 Mutants: the Role of Second Coordination Sphere Residues in the Regulation of Enzyme Activity [†]. Biochemistry (Mosc.) 42, 7294–7302.

(43). Segraves EN, Chruszcz M, Neidig ML, Ruddat V, Zhou J, Wecksler AT, Minor W, Solomon EI, and Holman TR (2006) Kinetic, Spectroscopic, and Structural Investigations of the Soybean Lipoxygenase-1 First-Coordination Sphere Mutant, Asn694Gly [†, ‡]. Biochemistry (Mosc.) 45, 10233–10242.

(44). Lu X, Liu S, Feng Y, Rao S, Zhou X, Wang M, Du G, and Chen J (2014) Enhanced thermal stability of Pseudomonas aeruginosa lipoxygenase through modification of two highly flexible regions. Appl. Microbiol. Biotechnol 98, 1663–1669. [PubMed: 23793260]

(45). Hsi LC, Wilson LC, and Eling TE (2002) Opposing Effects of 15-Lipoxygenase-1 and −2 Metabolites on MAPK Signaling in Prostate: ALTERATION IN PEROXISOME PROLIFERATOR-ACTIVATED RECEPTOR. J. Biol. Chem 277, 40549–40556. [PubMed: 12189136]

(46). O'Flaherty JT, Hu Y, Wooten RE, Horita DA, Samuel MP, Thomas MJ, Sun H, and Edwards IJ (2012) 15-Lipoxygenase Metabolites of Docosahexaenoic Acid Inhibit Prostate Cancer Cell Proliferation and Survival. PLoS ONE (Maya-Monteiro CM, Ed.) 7, e45480. [PubMed: 23029040]

(47). Brash AR, Boeglin WE, and Chang MS (1997) Discovery of a second 15S-lipoxygenase in humans. Proc. Natl. Acad. Sci 94, 6148–6152. [PubMed: 9177185]

(48). Ringholz FC, Buchanan PJ, Clarke DT, Millar RG, McDermott M, Linnane B, Harvey BJ, McNally P, and Urbach V (2014) Reduced 15-lipoxygenase 2 and lipoxin A4/leukotriene B4 ratio in children with cystic fibrosis. Eur. Respir. J 44, 394–404. [PubMed: 24696116]

(49). Garreta A, Val-Moraes SP, Garcia-Fernandez Q, Busquets M, Juan C, Oliver A, Ortiz A, Gaffney BJ, Fita I, Manresa A, and Carpena X (2013) Structure and interaction with phospholipids of a prokaryotic lipoxygenase from Pseudomonas aeruginosa. FASEB J. 27, 4811–4821. [PubMed: 23985801]

(50). Brinckmann R, Schnurr K, Heydeck D, Rosenbach T, Kolde G, and Kühn H (1998) Membrane translocation of 15-lipoxygenase in hematopoietic cells is calcium-dependent and activates the oxygenase activity of the enzyme. Blood 91, 64–74. [PubMed: 9414270]

(51). Hunter JA, Finkbeiner WE, Nadel JA, Goetzl EJ, and Holtzman MJ (1985) Predominant generation of 15-lipoxygenase metabolites of arachidonic acid by epithelial cells from human trachea. Proc. Natl. Acad. Sci 82, 4633–4637. [PubMed: 3927287]

(52). Nadel JA, Conrad DJ, Ueki IF, Schuster A, and Sigal E (1991) Immunocytochemical localization of arachidonate 15-lipoxygenase in erythrocytes, leukocytes, and airway cells. J. Clin. Invest 87, 1139–1145. [PubMed: 2010530]

(53). Kuhn H, Wiesner R, Alder L, Fitzsimmons BJ, Rokach J, and Brash AR (1987) Formation of lipoxin B by the pure reticulocyte lipoxygenase via sequential oxygenation of the substrate. Eur. J. Biochem 169, 593–601. [PubMed: 3121318]

(54). Levy BD, Romano M, Chapman HA, Reilly JJ, Drazen J, and Serhan CN (1993) Human alveolar macrophages have 15-lipoxygenase and generate 15(S)-hydroxy-5,8,11-cis-13-trans-eicosatetraenoic acid and lipoxins. J. Clin. Invest 92, 1572–1579. [PubMed: 8376607]

(55). Deschamps JD, Gautschi JT, Whitman S, Johnson TA, Gassner NC, Crews P, and Holman TR (2007) Discovery of platelet-type 12-human lipoxygenase selective inhibitors by high-throughput screening of structurally diverse libraries. Bioorg. Med. Chem 15, 6900–6908. [PubMed: 17826100]

(56). Rai G, Kenyon V, Jadhav A, Schultz L, Armstrong M, Jameson JB, Hoobler E, Leister W, Simeonov A, Holman TR, and Maloney DJ (2010) Discovery of Potent and Selective Inhibitors of Human Reticulocyte 15-Lipoxygenase-1. J. Med. Chem 53, 7392–7404. [PubMed: 20866075]

(57). Jameson JB, Kantz A, Schultz L, Kalyanaraman C, Jacobson MP, Maloney DJ, Jadhav A, Simeonov A, and Holman TR (2014) A High Throughput Screen Identifies Potent and Selective Inhibitors to Human Epithelial 15-Lipoxygenase-2. PLoS ONE (Jung M, Ed.) 9, e104094. [PubMed: 25111178]

(58). Luci DK, Jameson JB, Yasgar A, Diaz G, Joshi N, Kantz A, Markham K, Perry S, Kuhn N, Yeung J, Kerns EH, Schultz L, Holinstat M, Nadler JL, Taylor-Fishwick DA, Jadhav A, Simeonov A, Holman TR, and Maloney DJ (2014) Synthesis and Structure–Activity Relationship Studies of 4-((2-Hydroxy3-methoxybenzyl)amino)benzenesulfonamide Derivatives as Potent and Selective Inhibitors of 12-Lipoxygenase. J. Med. Chem 57, 495–506. [PubMed: 24393039]

(59). Vasquez-Martinez Y, Ohri RV, Kenyon V, Holman TR, and SepúlvedaBoza S (2007) Structure–activity relationship studies of flavonoids as potent inhibitors of human platelet 12-hLO, reticulocyte 15-hLO-1, and prostate epithelial 15-hLO-2. Bioorg. Med. Chem 15, 7408–7425. [PubMed: 17869117]

(60). Starkey M, Hickman JH, Ma L, Zhang N, De Long S, Hinz A, Palacios S, Manoil C, Kirisits MJ, Starner TD, Wozniak DJ, Harwood CS, and Parsek MR (2009) Pseudomonas aeruginosa Rugose Small-Colony Variants Have Adaptations That Likely Promote Persistence in the Cystic Fibrosis Lung. J. Bacteriol 191, 3492–3503. [PubMed: 19329647]

(61). Hickman JW, Tifrea DF, and Harwood CS (2005) A chemosensory system that regulates biofilm formation through modulation of cyclic diguanylate levels. Proc. Natl. Acad. Sci. U. S. A 102, 14422–14427. [PubMed: 16186483]

(62). Moreau-Marquis S, Bomberger JM, Anderson GG, Swiatecka-Urban A, Ye S, O'Toole GA, and Stanton BA (2008) The F508-CFTR mutation results in increased biofilm formation by Pseudomonas aeruginosa by increasing iron availability. AJP Lung Cell. Mol. Physiol 295, L25–L37.

(63). Neidig ML, Wecksler AT, Schenk G, Holman TR, and Solomon EI (2007) Kinetic and Spectroscopic Studies of N694C Lipoxygenase: A Probe of the Substrate Activation Mechanism of a Nonheme Ferric Enzyme. J. Am. Chem. Soc 129, 7531–7537. [PubMed: 17523638]

(64). Hoobler EK, Rai G, Warrilow AGS, Perry SC, Smyrniotis CJ, Jadhav A, Simeonov A, Parker JE, Kelly DE, Maloney DJ, Kelly SL, and Holman TR (2013) Discovery of a Novel Dual Fungal CYP51/Human 5-Lipoxygenase Inhibitor: Implications for Anti-Fungal Therapy. PLoS ONE (Nie D, Ed.) 8, e65928. [PubMed: 23826084]
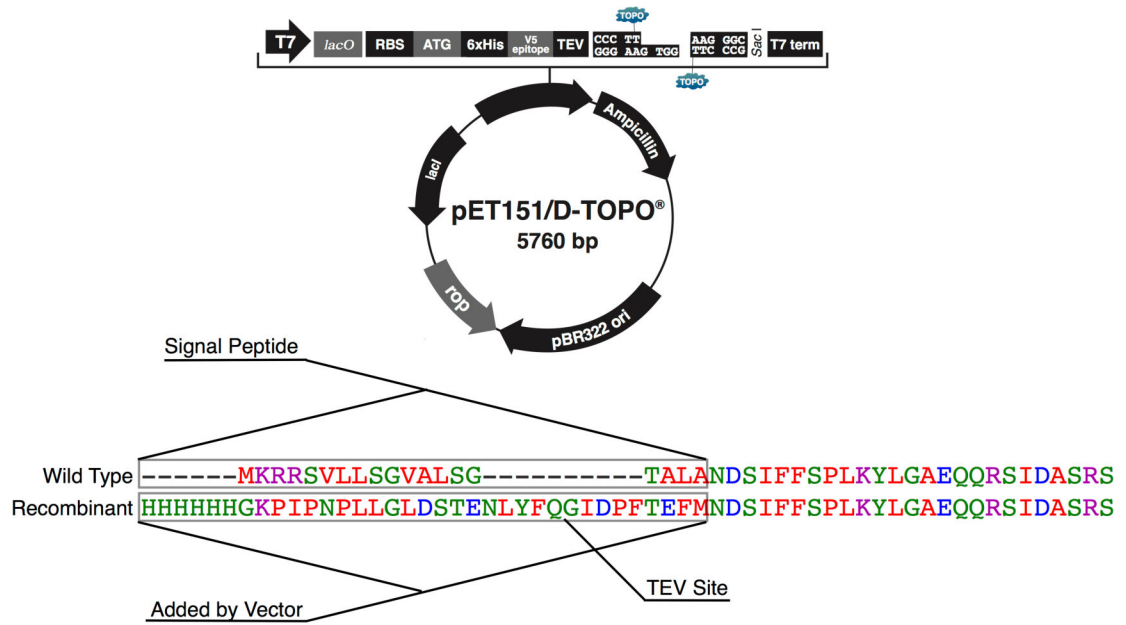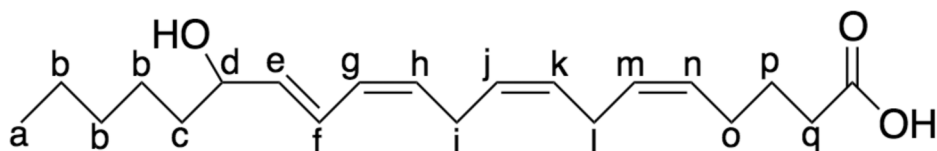
Figure 1.
Signal peptide and vector added sequences of wild type and recombinant LoxA protein

Label	15-HETE		R-Mosher		S-Mosher		u (S-R)
a	0.89	t	0.81	t	0.84	s	0.038
b	1.30	m	1.19	m	1.26	m	0.063
c	1.55	m	1.58	m	1.62	m	0.047
d	4.27	p	5.51	qa	unc	--	--
e	5.71	dd	5.61	dd	5.50	m	-0.107
f	6.61	dd	6.61	dd	6.53	t	-0.073
g	5.99	m	5.95	t	5.91	t	-0.037
h	5.40	m	5.44	qa	5.41	m	-0.033
i	2.99	m	2.91	t	2.87	t	-0.033
j	5.40	m	5.32	m	5.32	m	-0.002
k	5.40	m	unc	--	unc	--	--
l	2.83	s	2.76	t	2.77	t	0.007
m	5.40	m	unc	--	unc	--	--
n	5.40	m	5.32	m	5.33	m	0.008
o	2.14	m	2.11	qa	2.11	qa	0.003
p	1.69	m	1.70	m	1.71	m	0.008
q	2.34	s	2.42	t	2.43	t	0.004

Figure 2.
Chemical shift values of carbon atoms in 15-HETE, generated by LoxA. Splitting: s; singlet, d; doublet, t; triplet, qa; quartet, qi; quintet, m; multiplet, dd; doublet of doublets. unc: exact position unclear
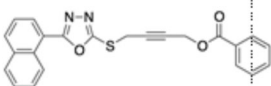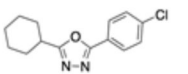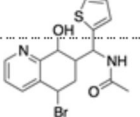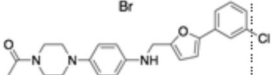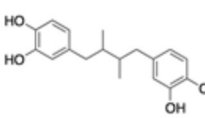
Compound	Specificity	Structure	IC_{50} (μM) [± SD (μM)]	% I at 25 μM for LoxA	~IC_{50} (μM) for LoxA	Fold difference In IC_{50}
24	15-LOX-1		0.01 [0.01]	34	20.	2000
MLS000545091	15-LOX-2		2.6 [0.4]	11	78	30
5	12-LOX		1.0 [0.2]	1	>100	>100
13	5-LOX		0.52 [0.07]	18	46	100
N/A	N/A (redox)		0.1-10	79	11 [1]	--

Figure 3.
Various specific human LOX inhibitors were assayed against LoxA to determine their potency. Potency difference was calculated using estimated IC_{50} for LoxA divided by previously published IC_{50} for human isozyme.[56–58,64]

Figure 4.
Western blot for LoxA showing LOX expression in various strains under planktonic and biofilm growth conditions. Strains: WS, WspF knockout of PAO1; WT, PAO1; KO, *loxA* transposon knockout of PAO1; OV, PAO1 carrying pBadLOX, PA1168 and PA1169 overexpression vector; OI, Same as OV, induced with 0.5% arabinose; PP, Purified recombinant LoxA, 100 ng.
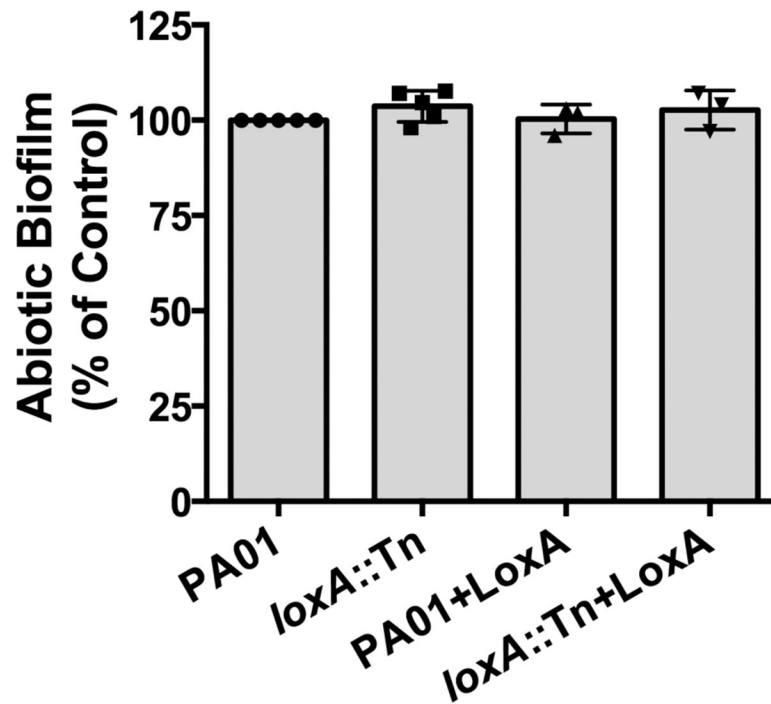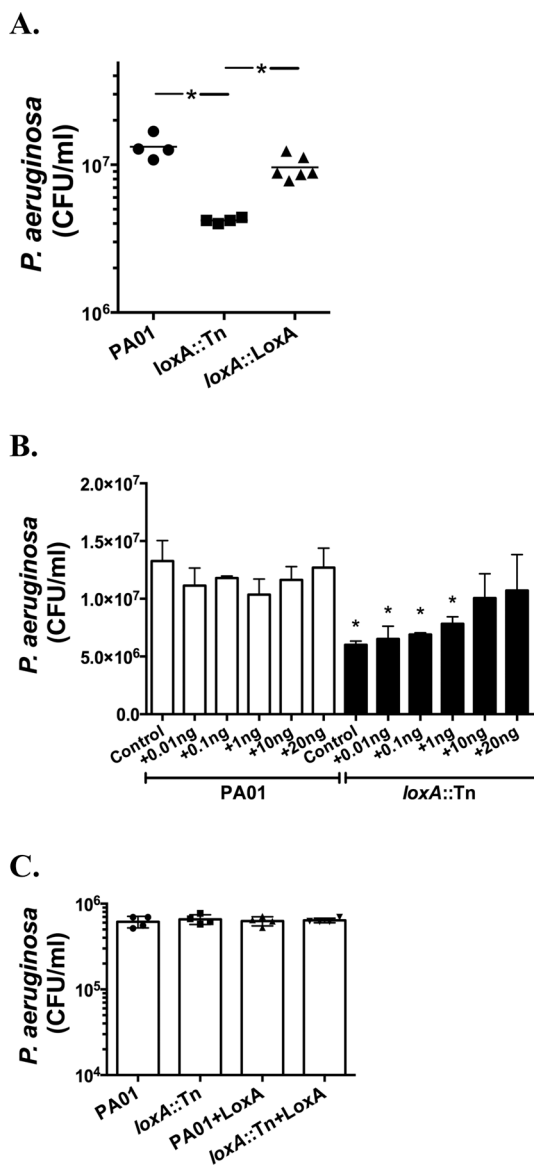
Figure 5.
Abiotic biofilm assay showing P. aeruginosa biofilm growth for *loxA* mutant and reconstitution with recombinant LoxA protein. Using a microtiter biofilm assay, biofilm growth was compared for wild-type PAO1 *P. aeruginosa*, *loxA*::Tn in PAO1, PAO1 + 1μg LoxA protein and *loxA*::Tn + 1 μg LoxA protein to complement. Biofilm growth was normalized to wild-type PAO1 biofilm growth. All experiments were performed at least three times.

A.

B.

C.

Figure 6.
Biotic biofilm assays for loxA mutant *P. aeruginosa*. A) P*. aeruginosa* biofilm growth on human airway epithelial cells was compared for wild-type PAO1, *loxA*::Tn mutant and *loxA*::LoxA complemented strains. Bacterial biofilm growth was quantified by enumerating colony-forming units (CFU/ml). Experiments performed four times. *p<0.001. B) P*. aeruginosa* biofilms were grown on human airway epithelial cells for wild-type PAO1 and the *loxA*::Tn mutant and reductions in biofilm growth in the loxA:: Tn mutant were rescued with increasing doses of LoxA protein. Bacterial biofilm growth was quantified by enumerating colony-forming units (CFU/ml). Experiments performed three times. *p<0.01. C) Attachment assays were performed to assess the attachment of wild-type and *loxA*::Tn mutant *P. aeruginosa* to human airway epithelial cells, in the presence and absence of LoxA protein addition. Attached bacteria at one hour post-inoculation were quantified by enumerating colony-forming units (CFU/ml). Experiments were performed four times.

Table 1.

Pairwise sequence alignment statistics for selected LOX enzymes with LoxA.

Protein	Mol Wt (kD)	Identity	Similarity	Gaps	Score
LoxA	74.81	--	--	--	--
s15-LOX-1	94.38	23.9%	37.3%	22.4%	20.00
5-LOX	78.00	27.1%	42.5%	8.5%	23.57
12-LOX	75.71	23.5%	37.8%	7.8%	20.39
15-LOX	74.82	24.7%	39%	9.9%	19.36
15-LOX-2	75.87	26.2%	40.8%	6.4%	24.77

Table 2.

Kinetic parameters for LoxA, determined at multiple pH values.

pH	K_{cat} (s^{-1})	K_m (μM)	K_{cat} $/K_m$ $(\mu M^{-1}s^{-1})$
6.5	181(6)	12(1)	16(2)
7.0	157(5)	12(1)	13(1)
7.5	86(2)	13(1)	6.6(0.6)

Table 3.

Kinetic parameters for LoxA at pH of maximal activity compared to selected 15-LOX enzymes at their maximal activities. Kinetic parameters for s15-LOX-1,[63] 15-LOX-1[41] and 15-LOX-2[41] were published previously.

Enzyme	K_{cat} (s^{-1})	K_{cat} /K_m ($\mu M^{-1}s^{-1}$)
LoxA	181 (6)	16 (2)
s15-LOX-1	287 (5)	19 (1)
15-LOX-l	5.3 (0.4)	2.0 (0.2)
15-LOX-2	0.74 (0.03)	0.1 (0.01)

Table 4.

LoxA substrates ordered by maximum turnover rate as a percentage of the fastest substrate (AA). Products made by each substrate were determined with approximate percentage of total product shown. N/D: not determined

Substrate	% AA Rate (10 μM)	Product	Approximate % of total
AA	100	15-HETE	94
		9-HETE	6
		11-HETE	<1
ALA	78(10)	13-HOTrE	91
		N/D	9
LA	72(10)	13-HODE	93
		9-HODE	4
DHA	72(10)	17-HDoHE	93
		4-HDoHE	7
		20-HDoHE	<1
EPA	61(10)	15-HEPE	78
		18-HEPE	14
		11-HEPE	8
DGLA	44(10)	15-HETrE	100
GLA	44(10)	13-HOTrE(ϒ)	78
		N/D	20
		N/D	2
EDA	33(10)	15-HEDE	70
		11-HEDE	30

Table 5.

Comparison of peroxidating ability of LoxA to selected human LOX enzymes with phosphoester linked substrate, in the presence and absence of calcium.

Enzyme	AA Act/ μg	PC-AA Act/ μg	%PC-AA/AA Ratio - Ca	PC-AA +Ca Act/ μg	%PC-AA/AA Ratio + Ca
15-LOX-1	25	0.08	0.31	0.51	2.1
15-LOX-2	0.86	0.03	4.1	0.05	6.3
12-LOX	2.5	0.02	0.97	0.02	0.96
LoxA	40	0.09	0.22	0.14	0.35

Table 6.

Comparison of kinetic parameters for LoxA with LA and perdeuterated LA to determine the KIE.

Substrate	K_{cat} (s^{-1})	K_m (μM^{-1})	K_{cat} /K_m ($\mu M^{-1}s^{-1}$)
LA	28 (2)	7 (2)	3.8 (0.9)
d31-LA	0.9 (0.1)	100 (24)	0.009 (0.002)
KIE	32 (6)		450 (70)

Table 7.

K_{cat} comparison of secondary products relative to AA. The relative Kcat of LoxA with A.A is set to 1. All other K_{cat} values are standardized to this value and are unitless.

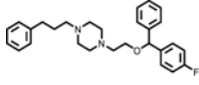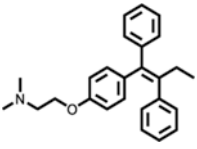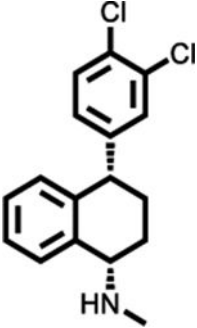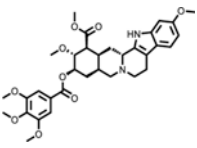| Substrate	Relative K_{cat}
AA	1
15-HpETE	$1e^{-4}$
15-HETE	$1e^{-5}$
5-HpETE	$1e^{-5}$
5-HETE	$1e^{-5}$
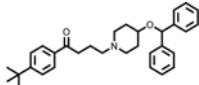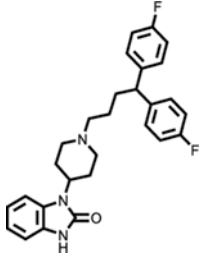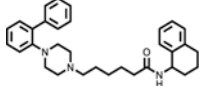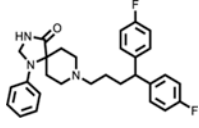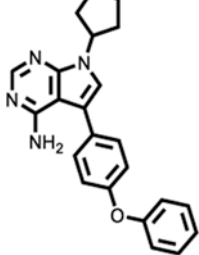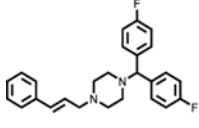
Table 8.

LoxA single-point screen inhibition percentages. Compounds are listed relative to their percent potency towards LoxA, with the most potent listed first. Each reaction contained 10 μM of A.A. and 25 μM inhibitor.

Inhibitor	LoxA	15-LOX-l	12-LOX	5-LOX	15-LOX-2
NCGC00164603	95%	76%	33%	23%	0%
NCGC00015802	90%	69%	50%	80%	16%
NCGC00186032	87%	57%	36%	78%	5%
NCGC00015424	87%	76%	63%	74%	21%
NCGC00015280	86%	51%	38%	42%	0%
NCGC00018102	86%	65%	25%	96%	0%
NCGC00015300	83%	65%	48%	41%	13%
NCGC00024928	82%	73%	39%	79%	8%
NCGC00092386	76%	51%	26%	83%	5%
NCGC00091250	69%	57%	23%	37%	5%

Table 9.

LoxA IC50 inhibitor values. Compounds are listed relative to their potency towards LoxA, with the most potent listed first.

	Inhibitor	IC$_{50}$ (μM)
	NCGC00164603	10.1 ± 3.3
	NCGC00015802	5.8 ± 1.4
	NCGC00186032	11.4 ± 1.9
	NCGC00015424	4.1 ±1.4
	NCGC00015280	16.2 ± 3.1
	NCGC00018102	4.5 ± 0.4
	NCGC00015300	8.0 ± 1.2

	Inhibitor	IC$_{50}$ (μM)
	NCGC00024928	6.7 ± 1.4
	NCGC00092386	13.1 ± 1.7
	NCGC00091250	13.8 ± 4.2